International Journal of Heat and Mass Transfer 52 (2009) 2484–2497

Contents lists available at ScienceDirect

International Journal of Heat and Mass Transfer

journal homepage: www.elsevier.com/locate/ijhmt

Performance predictions of laminar and turbulent heat transfer and fluid flow of heat exchangers having large tube-diameter and large tube-row by artificial neural networks

Gongnan Xie [a,b], Bengt Sunden [b,*], Qiuwang Wang [a,1], Linghong Tang [a]

[a] State Key Laboratory of Multiphase Flow in Power Engineering, School of Energy and Power Engineering, Xi'an Jiaotong University, Xi'an 710049, PR China
[b] Division of Heat Transfer, Department of Energy Sciences, Lund University, P.O. Box 118, SE-221 00 Lund, Sweden

ARTICLE INFO

Article history:
Received 15 February 2008
Available online 5 March 2009

Keywords:
Heat transfer
Friction
Artificial neural network (ANN)
Large tube-diameter and large number of tube rows
Correlations

ABSTRACT

In this work an artificial neural network (ANN) is used to correlate experimentally determined and numerically computed Nusselt numbers and friction factors of three kinds of fin-and-tube heat exchangers having plain fins, slit fins and fins with longitudinal delta-winglet vortex generators with large tube-diameter and large the number of tube rows. First the experimental data for training the network was picked up from the database of nine samples with tube outside diameter of 18 mm, number of tube rows of six, nine, twelve, and Reynolds number between 4000 and 10,000. The artificial neural network configuration under consideration has twelve inputs of geometrical parameters and two outputs of heat transfer Nusselt number and fluid flow friction factor. The commonly-implemented feed-forward back propagation algorithm was used to train the neural network and modify weights. Different networks with various numbers of hidden neurons and layers were assessed to find the best architecture for predicting heat transfer and flow friction. The deviation between the predictions and experimental data was less than 4%. Compared to correlations for prediction, the performance of the ANN-based prediction exhibits ANN superiority. Then the ANN training database was expanded to include experimental data and numerical data of other similar geometries by computational fluid dynamics (CFD) for turbulent and laminar cases with the Reynolds number of 1000–10,000. This in turn indicated the prediction has a good agreement with the combined database. The satisfactory results suggest that the developed ANN model is generalized to predict the turbulent or/and laminar heat transfer and fluid flow of such three kinds of heat exchangers with large tube-diameter and large number of tube rows. Also in this paper the weights and biases corresponding to the neural network architecture are provided so that future research can be carried out. It is recommended that ANNs might be used to predict the performances of thermal systems in engineering applications, especially to model heat exchangers for heat transfer analysis.

1. Introduction

A heat exchanger is such an equipment that the process of heat or/and mass exchange between two and more steams at different temperatures occurs. For saving energy and resources, it is essential to increase the thermal performance of heat exchangers. Generally, it is an effective way to employ extended surfaces (or referred to as finned surfaces) on the gas side to compensate for the low heat transfer coefficient, which maybe 10-to-100 times smaller than that on the liquid-side, meaning that the dominant resistance is usually on the gas side. Fin-and-tube heat exchangers (FTHEs) are such kinds of heat exchangers having mechanically (or hydraulically) expanded round tubes in a block of parallel continuous fins with one or more rows, as sketched in Fig. 1. FTHEs are extensively employed in chemical engineering and HVAC&R (heating, ventilation and air conditioning, refrigeration) applications such as compressor intercoolers, air-coolers and fan coils. Adoption of finned surfaces is to disturb the pattern of flow and destroy the boundary layer. Accordingly, to satisfy the desire to enhance heat transfer, a variety of finned surfaces has been developed and applied successfully. These finned surfaces include crimped spiral fin, plain fin, slotted fin, louvered fin and fin with delta-wing longitudinal vortex generator, etc. Therefore, performance data of heat transfer and friction factor for these finned surfaces for fin-and-tube heat exchangers is very important for accurate compact heat exchanger design [1–3]. Many efforts are devoted on experimental studies and numerical computations of FTHEs, and lots of useful results and correlations have been presented. Typical references are qualified by [4–9].

* Corresponding author. Tel.: +46 46 2228605; fax: +46 46 2224717.
E-mail addresses: Gongnan.Xie@energy.lth.se (G. Xie), Bengt.Sunden@energy.lth.se (B. Sunden), wangqw@mail.xjtu.edu.cn (Q. Wang).
[1] Tel./fax: +86 29 82663502.

0017-9310/$ - see front matter © 2009 Elsevier Ltd. All rights reserved.
doi:10.1016/j.ijheatmasstransfer.2008.10.036

Nomenclature

A	output variable of ANN
b	bias of ANN neuron
D_c	fin collar outside diameter, $D_c = D_o + 2\delta_f$ (mm)
D_i	inside diameter of tube (mm)
D_o	outside diameter of tube (mm)
Er	absolutely relative error (%)
F_p	fin pitch (mm)
F_s	fin distance (mm)
f	friction factor
M	number of sets of data for training
N_t	number of tube rows
N	number of sets of data for testing
Nu	Nusselt number
P_l	longitudinal tube pitch (mm)
Pr	Prandtl number
P_t	transverse tube pitch (mm)
rms	root-mean-squares error
R	definition by Eq. (9a)
Re	Reynolds number, $Re_{D_c} = \rho v D_c/\mu$
S_h	height of slit (mm)
S_l	length of slit (mm)
S_w	width of slit (mm)
V_h	height of vortex generator (mm)
V_l	length of vortex generator (mm)
u	the net input by adding all the inputs
w	weight matrix of ANN connections

Greek symbols

α	angle of attack (deg)
δ_f	fin thickness (mm)
σ	definition by Eq. (9b)
φ	activation function
Δp	pressure drop (Pa)

Superscripts

c	numerical data
e	experimental data
p	prediction by ANN

In order to evaluate the heat exchanger performances, efficient and accuracy methods for prediction of heat transfer and pressure drop have to be developed. The computational intelligence techniques, such as artificial neural networks (ANNs), genetic algorithms (GAs), fuzzy logic, have been successfully applied in many scientific researches and engineering practices. ANNs have been developed for about two decades and are now widely used in various application areas such as performance prediction, pattern recognition, system identification, and dynamic control and so on, since ANNs provide better and more reasonable solutions. ANN offers a new way to simulate nonlinear, or uncertain, or unknown complex systems without requiring any explicit knowledge about input–output relationship. ANN has more attractive advantages. It can approximate any continuous or nonlinear function by using certain network configuration. It can be used to learn complex nonlinear relationship from a set of associated input–output vectors. It can be implemented to dynamically simulate and control unknown or uncertain processes. In recent years, ANNs have been used in thermal systems for heat transfer analysis, performance prediction and dynamic control of heat exchangers [10–25]. For example, Yang and Sen [10] and San and Yang [11] reviewed works in dynamic modeling and controlling of heat exchangers using ANNs and GAs. Two interesting examples were presented to support the superiority of ANNs and GAs compared to correlations. Diaz et al. [12–15] did lots of work in steady and dynamic simulation and control of a single-row fin-and-tube heat exchanger using ANNs. Pacheco-Vega et al. [16,17] also made heat transfer analysis for a fin-tube heat exchanger based on limited experimental data with air and R22 as fluids, and predicted heat transfer rates of air–water heat exchangers using soft computing and global regression. Islamoglu et al. [18,19] predicted heat transfer rate for a wire-on-tube heat exchanger and predicted outlet temperature and mass flow rate for a non-adiabatic capillary tube suction line heat exchanger. Xie et al. [20] and Wang et al. [21] conducted heat transfer analysis and performance prediction of shell-and-tube heat exchangers with helical baffles based on their experimental data. Ertunc et al. [22–24] conducted neural networks analysis and prediction of an evaporative condenser, a cooling tower, a cooling coil. Zdaniuk et al. [25] combined their data and other databases to predict the performance of helically finned tubes by a single-output ANN. Beside for heat exchanger applications, other applications of artificial neural networks for heat transfer analysis and fluid flow process predictions can be found in [26–32]. From the aforementioned successful applications, it is shown that ANNs

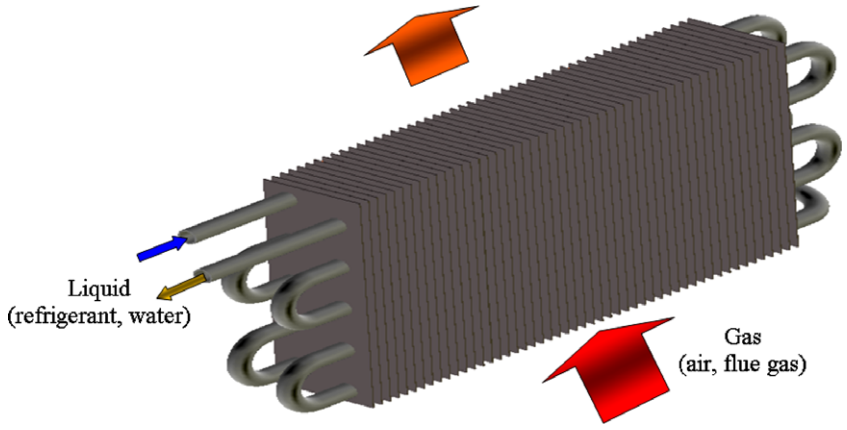

Fig. 1. A typical fin-and-tube heat exchanger (a liquid flows into the tubes and a gas flows across the finned-tube bundle).

are efficient techniques for estimation or prediction of heat transfer and fluid flow process, and are well suitable to thermal analysis in engineering systems, especially in heat exchangers.

In the above-mentioned literature, most works were done in thermal analysis focusing on fin-and-tube heat exchangers with small numbers of tube rows (mostly less than 4) or small tube-diameter (mostly in the range of 8–13 mm), which are commonly used in the HVAC&R engineering, or shell-and-tube heat exchangers, e.g., [12–17]. However, ANNs have not yet been applied to correlate and predict heat transfer and flow friction of fin-and-tube heat exchangers with large number of tube rows and large tube-diameter. In some certain industrial applications of large industry, such as intercoolers of multi-stage compressors employed in high pressure and temperature plants like gas turbine plant, the number of tube rows (might be larger than 4 or much larger) and the outside diameter of the tubes is large (might be larger than 13 mm or much larger). The intercooler is so used that the cooling air at compressor intake results in decrease of compressor work and thereby increase of the net work output of plants. Most of the above-mentioned ANN configurations only have a single output, e.g., [18–21,25–32], which will lead to more sets of networks should be developed for different output. For this reason, the objective of this paper is to develop and apply an ANN for heat transfer analysis of fin-and-tube heat exchangers having large tube-diameter and large number of tube rows with experimental data based on the back propagation algorithm for training the network. Different network configurations were studied to search an optimal network configuration for prediction. Then, the ANN was again trained with the combined database from the experimental data and numerical data by computational fluid dynamics (CFD) for turbulent cases, and finally the ANN was secondly trained by the combined database of experimental data and numerical data from turbulent and laminar computations. This paper extends the work in paper [33], where only turbulent heat transfer and fluid flow were correlated using an ANN. Although the ANN methodology is not new, the present work contributes to application of ANN in such heat exchangers.

2. Experimental data and FTHEs geometry

FTHE is one of the successful improvements of the tubular heat exchanger. As shown in Fig. 1, the hot air or flue gas flows across a finned tube bundle while cold water or refrigerant flows inside the round tubes that are arranged staggered. The heat is transmitted through the tube wall and finned surfaces. Fin patterns are diversified as varying their geometries. The common types are plain fins, wavy fins, slotted fins, louvered fins and fins with longitudinal vortex generators (LVGs). On the other side, the common types of tubes are round, flat and oval. The heat transfer and pressure drop characteristics on the air side can be obtained by experimental measurements or exact numerical computations. Fortunately, much literature has contributed to FTHEs and established most useful correlations.

Experiments have been conducted to measure convective heat transfer and pressure drop of FTHEs with large number of large-diameter tube rows by Tang et al. [34–36] at Xi'an Jiaotong University, China. Nine samples of three kinds of fin-and-tube heat exchangers are tested, the types of fins are plain fin, slit fin, fin with longitudinal vortex generations (LVGs), and the number of tube rows are six, nine, and twelve, which may not commonly appear in HVAC&R. It should be emphasized that the outside diameter of the tube is 18 mm, which also is not used generally in refrigeration engineering. The detailed geometrical parameters are tabulated in Table 1 and schematically shown in Fig. 2 (hereafter, the fins with LVGs are called LVG fins). All tubes and fins are made of copper. The tubes are in staggered arrangement. The thickness of fin is 0.3 mm. Experiments were performed for Reynolds number ranging from 4000 to 10,000 on the air side where the flow might be considered in transition to turbulent flow. The experimental apparatus and procedures are described in details in [34–36].

Ninety-six sets of experimental data were obtained and divided into two parts: one is for training data, the rest is for testing data. Experimentally determined friction factors and Nusselt numbers are plotted in Fig. 3. The typical uncertainties of friction factor and Nusselt number are 8.5% and 6.9%, respectively. A total of 96 sets of data were run in the network, of which 75 sets of experimental data were used to train the network, while the rest of 21 sets of data were used to test the network. Note that 78% of the experimental data was used for training the network. The selection of test data from each heat exchanger may be somewhat arbitrary. However, these data are based on approximate uniform variation of Re and based on total number of data points from each heat exchanger.

Tang et al. [34–36] also correlated their experimental data, as shown in Fig. 3, in the following forms.

For plain fins

$$Nu = 0.080Re^{0.71} \tag{1a}$$

$$f = 12.83Re^{-0.36} \tag{1b}$$

For slit fins

$$Nu = 0.057Re^{0.77} \tag{2a}$$

$$f = 13.28Re^{-0.35} \tag{2b}$$

For LVG fins

$$Nu = 0.094Re^{0.71} \tag{3a}$$

$$f = 10.68Re^{-0.34} \tag{3b}$$

Tang et al. [34] stated that the Eqs. (1–3) were shown to correlate the experimental data well. Also, these correlations can be referred to engineering applications or further research such as optimizations or predictions.

3. Neural network configuration

An ANN consists of a great number of interconnected neurons. A block diagram of the model of a neuron is shown in Fig. 4. A neuron is a basic information processing and operating unit in a neural network. Specifically, a signal x_i is input to connect to a neuron with the synaptic weight w_i, and then all input signals weighted by their respective synapses are summed as a net input u. A bias b is applied to the neuron so that the increase or decrease of net input depends on whether the bias is positive or negative. Finally the increased or decreased net input is imported into an activation

Table 1
Geometric parameters of the fin-and-tube heat exchangers.

Type	D_i	D_o	D_c	F_p	P_t	P_l	S_w	S_l	S_h	V_l	V_h	α	N
Plain	16	18	18.6	3.2	42	34	–	–	–	–	–	–	6,9,12
Slit	16	18	18.6	3.2	42	34	2.2	16	1.0	–	–	–	6,9,12
LVG	16	18	18.6	3.2	42	34	–	–	–	5	1.85	45	6,9,12

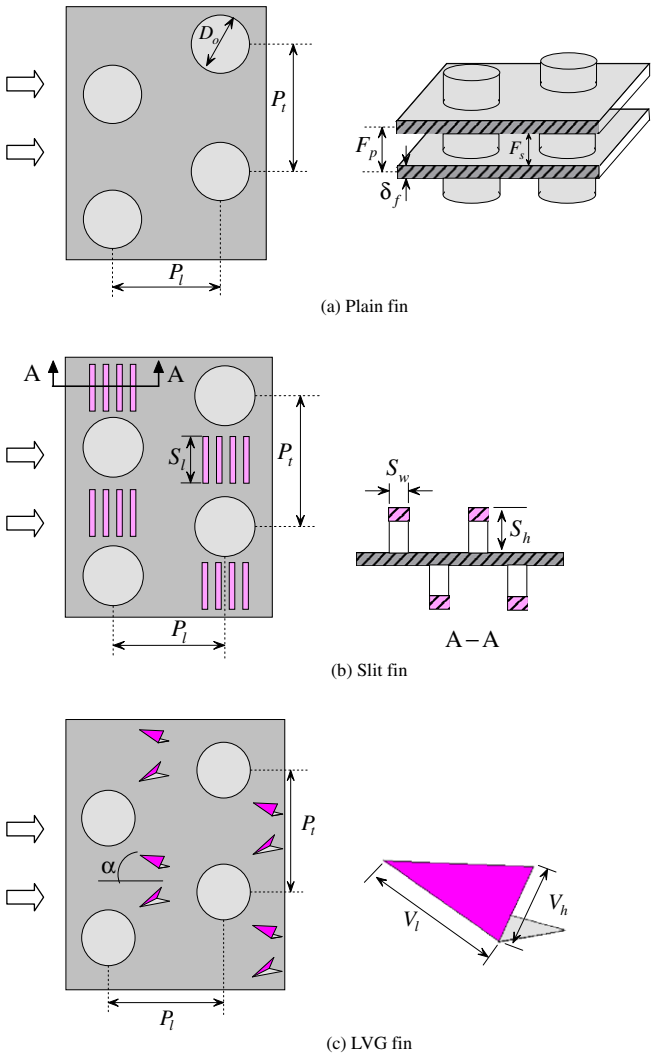

Fig. 2. Schematic sketch of fin patterns for fin-and-tube heat exchanger.

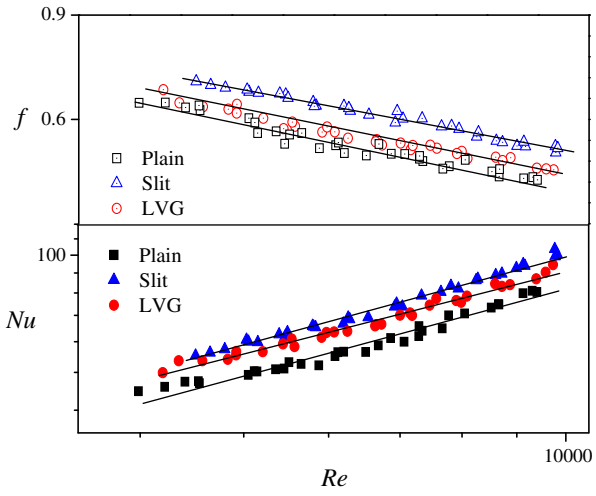

Fig. 3. Experimentally measured friction factors and Nusselt numbers for the present study of training neural networks.

function resulting in the output. The activation function is so developed that the amplitude of the net output of a neuron is limited. The input-to-output operation of a neuron is formulized mathematically as follows

$$u^k = \sum_{i=1}^{m} w_i^k x_i \tag{4a}$$

$$y^k = \varphi(u^k + b^k) = \varphi\left(\sum_{i=1}^{m} w_i^k x_i + b^k\right) = \varphi\left(\sum_{i=0}^{m} w_i^k x_i\right) \tag{4b}$$

It is noted that the bias may be accounted for as a new input fixed at $x_0 = \pm 1$ with its weight b and then combined with the original inputs as a whole input. Therefore the above equation has been reformulated to combine inputs and bias by replacing subscript 1 with 0 as seen in the last term of the right-hand side of Eq. (4b).

Fig. 5 illustrates a typical full-connected network configuration. Such an ANN consists of a series of layers with a number of neurons (circle points in Fig. 5, in this paper called nodes referring to figure). Each connection between two neurons with a real value is called *weight*. Neurons are gathered together into a column called a *layer*. Among various types of ANNs, the *feed-forward or multilayer perception* neural network is widely used in engineering applications. The input information is propagated forward through the network, while the output error is back propagated through the networks for updating the weights. As shown in Fig. 5, the first layer with six neurons and last layer with two neurons are called *input layer* and *output layer*, respectively, while the others in the middle are called *hidden layers*. The configuration in Fig. 5 has one hidden layer with four neurons (such type is briefly written as 6-4-2 in this paper). There are many ways to design and implement ANNs. However, it is difficult to find an optimal network, considering the uniqueness of a real problem. Thus, a priori choice, such as selection of network topology, training algorithm and network size should be made based on experience in order to keep the task to a manageable proportion.

It is a very common way to use the back propagation (BP) algorithm to train artificial neural networks. The main idea of this algorithm is to minimize the *cost function* by the steepest descent method to add small changes in the direction of minimization. It simply consists of back-propagating the output errors to the network by modifying the weight matrices, that is, adding a correction weight Δw to a synaptic weight w. More descriptions of the BP algorithm can be found in references [10,11]. Varying the learning rate dynamically or using momentum terms can improve the convergence speed. The mathematical background, the procedures for training and testing the ANN, and description of the BP algorithm can be found in the reference [37]. Although the BP algorithm needs long time to converge, the algorithm has gained a remarkable popularity in the neural network community, since it is relatively easy to implement in engineering applications, as well as in thermal and energy applications, see [10–32]. Also the BP algorithm might provide solutions to large and difficult problems [37]. Thus in this study the BP is implemented to train the network.

For such kinds of fin-and-tube heat exchangers at hand, twelve independent parameters were fed into the input layer of the network: Reynolds numbers *Re*, the number of tube rows N_t, diameter of tube D_c, fin pitch F_p, tube pitches P_t and P_l, geometry of the slit fin S_w, S_l and S_h and geometry of the LVG fin V_l, V_h and α. The notations of geometrical parameters are illustrated in Fig. 2. The main reason for selection of these input variables is that the structure of the heat exchanger core due to the aforementioned differences between the three exchangers with different fins can be distinguished by these input parameters. For example, $S_w = S_l = S_h = 0$ for the plain fin and the LVG fin while $V_l = V_h = \alpha = 0$ for the plain fin and the slit fin. The effect of mass flow rate can be considered by the Reynolds number. The output layer contains two parameters: Nusselt number, *Nu*, and friction factor, *f*. It should be noticed

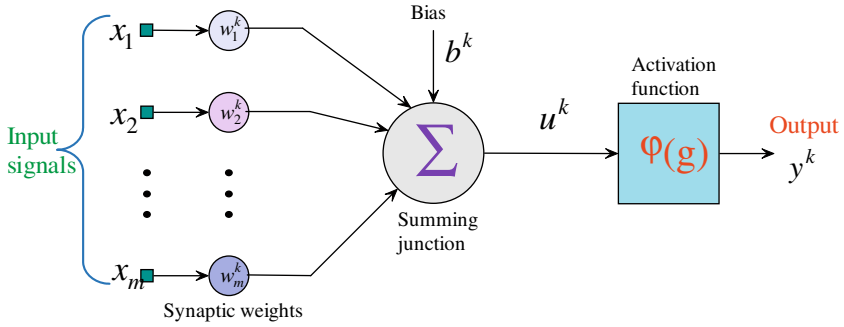

Fig. 4. Nonlinear model of a neuron.

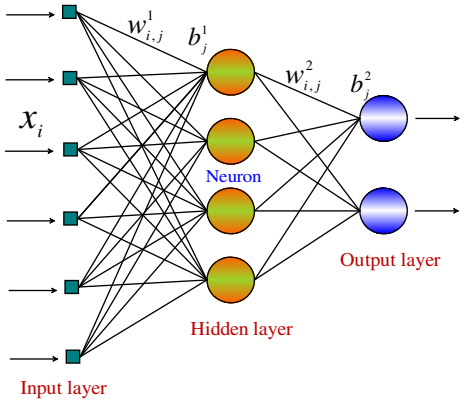

Fig. 5. A fully connected feed-forward neural network (the ANN having one hidden layer with four hidden neurons and one output layer with two outputs, briefly written as 6-4-2.

that the ANN prediction is off-line and is carried out after all experimental data have been reduced.

There are three basic types of activation functions: *Threshold function*, *Piecewise linear function* and *Sigmoid function* [37]. The forms of function are briefly re-written as follows.

$$\text{Threshold function}: \varphi(x) = \begin{cases} 1, & x \geqslant 0 \\ 0, & x < 0 \end{cases} \tag{5a}$$

$$\text{Piecewise linear function}: \varphi(x) = \begin{cases} 1, & x \geqslant 0.5 \\ x, & 0.5 > x > -0.5 \\ 0, & x \leqslant -0.5 \end{cases} \tag{5b}$$

$$\text{Sigmoid function}: \varphi(x) = \frac{1}{1+e^{-x}} \tag{5c}$$

In the present study, the popular *sigmoid* function was adopted in hidden layers and output layer. This is because such a function can exhibit a graceful balance between linear and nonlinear behavior, and it has a special characteristic feature of differentiability, which is an important feature for neural networks. Obviously, the net summation of input, $u + b$ in Eq. (4), is corresponded to x of the activation function, Eq. (5). In addition, it should be noted that the sigmoid function has the asymptotic limits of [0,1]. Consequently, it is desirable to normalize all the input–output data with the largest and smallest values of each of the data sets, since the variables of input–output data have different physical units and range sizes. Thus, to avoid any computational difficulty, all of the input–output pairs were normalized in [0.15,0.85] range based on previous experience [10–17]. That is, the input variables were scaled through the transformations:

$$x_i = \frac{x_i - x_{i,\min}}{x_{i,\max} - x_{i,\min}}(S_{\max} - S_{\min}) + S_{\min} \tag{6}$$

Here $S_{\max}$ and $S_{\min}$ are 0.85 and 0.15, respectively, $x_{i,\max}$ and $x_{i,\min}$ are the maximum and minimum values of individual input variable. So, even though original data is composed of dimensional unit and non-dimensional unit, the scaled input data is surely within the range of 0.15–0.85.

4. ANN development and assessment

In order to predict heat transfer and friction with high precision, attempts should be done to develop some ANN configurations and finally find a relative optimal or good configuration for prediction. As aforementioned, the drawback of the BP algorithm is that it may get stuck in a local minimum, and therefore the learning rate was changed during the training process of the network. In the present study, the learning rate was finally set to 0.4 based on previous experience [10–17]. On the other side, there are no well-defined criteria for convergence of the BP algorithm. It is a logical way to define such a criterion that the global maximum error is below an accepted level. In this study the training of the neural network was terminated when the maximum number of training cycles was reached, since the maximum relative error between the output of the network and the target output was less than 5% after a series of trial tests. Note that the selection of the number is a trial-and-error process in which it may be changed if the performance of the neural network during the training is not good enough. Finally, the number of training cycles was chosen to be 200,000. The relative error of every predicted output was defined by

$$Er = \frac{|A^e - A^p|}{A^e} \times 100\% \tag{7}$$

where A^p is the predicted results, that is output of ANN, A^e is the experimental data, that is the target output. The maximum error was determined by the maximum value of the maximum relative error of the two output variables.

During the training process of the neural network, the performance of the network was evaluated by calculating the root-mean-square (*rms*) values of the output error

$$rms = \sqrt{\frac{1}{M}\sum_{i=1}^{M}\left(\frac{A^e - A^p}{A^e}\right)^2} \tag{8}$$

M is the number of sets of data for training the neural network. The final *rms* error was determined by the maximum value of the *rms* error of the two output variables. As an example, the errors during training 12-9-5-2 network configuration with two hidden layers with 9 and 5 nodes, respectively, were shown in Fig. 6(a). It can be seen that the *maximum* error asymptotically reached at about 120,000 cycles, while the *rms* error is reached at 80,000 cycles. At the end of training process, the relative errors for the training data

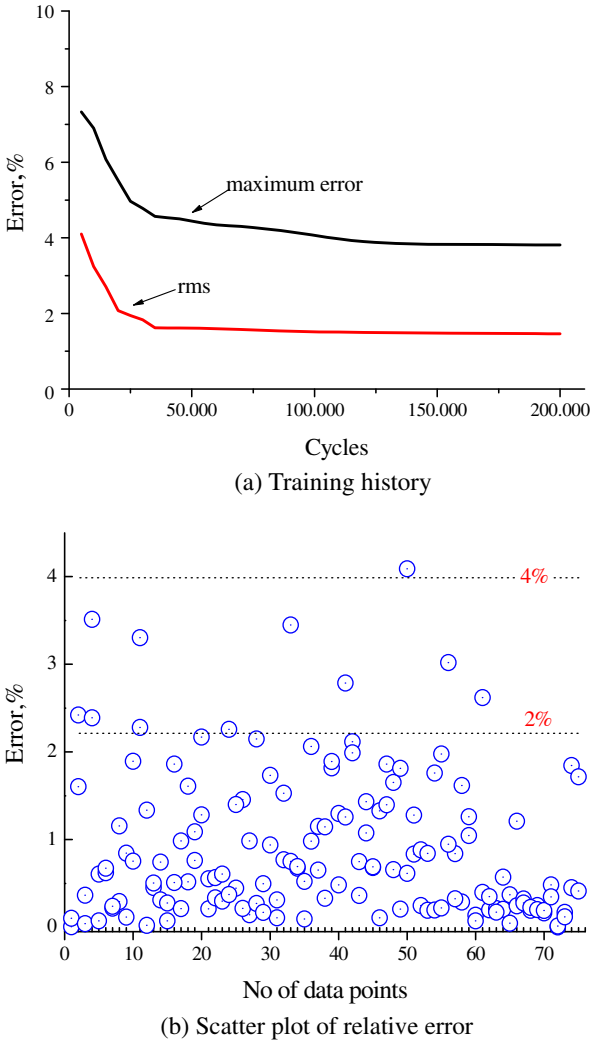

Fig. 6. Training process and error distribution of ANN 12-9-5-2.

were shown in Fig. 6(b). Most errors are within 2%, and the maximum relative error is about 4%.

Generalization is an ANN quality. It is the ability to provide accurate output results when the input data that have never been used for training is fed into the trained network. The network topology and size, such as selection of number of hidden layers and number of hidden nodes, will affect the predicted performance. Large networks can learn complex problems, but require more efforts and time to train and to report. Consequently, the selection process of a neural network configuration is a compromise between a principle that minimizes the prediction error and the network size keeping as small as possible. The performance of the trained network is evaluated by comparing its prediction with the data set aside for testing. Thus, in this study, by the aid of searching relatively good configuration for prediction, ten different ANN configurations were studied, as shown in Table 2. R and σ are defined by

$$R = \frac{1}{N}\sum_{i=1}^{N} R_i = \frac{1}{N}\sum_{i=1}^{N} \frac{A^e}{A^p} \tag{9a}$$

$$\sigma = \sqrt{\sum_{i=1}^{N} \frac{(R - R_i)^2}{N}} \tag{9b}$$

Table 2
Comparison of errors by different ANN configurations.

Configuration	Train error		Test error	
	Er (%)	*rms* (%)	*R*	σ
12-6-2	5.01623	1.67797	1.000348	0.004791
12-7-2	4.60366	1.56802	1.001196	0.004792
12-8-2	4.58049	1.15767	1.000517	0.004919
12-10-5-2	3.81628	1.43443	1.001223	0.006014
12-9-6-2	3.94815	1.40578	0.999446	0.007262
12-9-5-2	4.08936	1.44235	1.000385	0.004753
12-9-4-2	4.06629	1.54432	1.000615	0.006675
12-8-5-2	3.80853	1.46035	1.001296	0.004747
12-10-8-5-2	3.86046	1.37920	1.002111	0.004996
Correlations	8.04714	3.50697	0.994462	0.014185

Note: the error is the maximum value among the errors of the two output variables.

Note that in Table 2, R and σ are the maximum values which were determined from R and σ of the three output variables, respectively. R reflects the average accuracy of the prediction, while σ reflects the scatter of the prediction. Both quantities are important for an assessment of the relative success of the ANN analysis [10,11]. For three layers, when the number of hidden nodes is increased from 6 to 8, R and σ of the former are smaller than those of the latter. For four layers, when the number of hidden nodes of the first hidden layer is increased to 10 and the number of hidden nodes of the second hidden layer is increased to 5, R and σ become larger. This indicates that adding more hidden nodes may not improve the predicted results. From Table 2, 12-10-8-5-2 network own smaller *Er* and *rms* than those of 12-9-5-2, however, the R and σ of the former are larger than those of the latter. At this point, the configurations with four layers have higher prediction accuracy than those with five layers. It is also noted that adding more hidden layers may not make the prediction better. Thus, in this case, configuration 12-9-5-2 is selected for testing, with smallest R = 1.000385 and σ = 0.004753 and the maximum relative error is about 4% with most of them being less than 2% (see Fig. 6). The training process of different networks is shown in Fig. 7. Clearly, the training process of five layers 12-10-8-5-2 is so unstable that the relative error is involved, and although the error of three layers is smaller at the beginning stage than those of four layers, then the final error of the former is increased so as to be higher than at of the latter. Also, for the same number of layers, the training process of 12-9-5-2 is so smoothly decreasing while the process of the other two networks is somewhat increased resulting in slightly higher errors at the end of the training process.

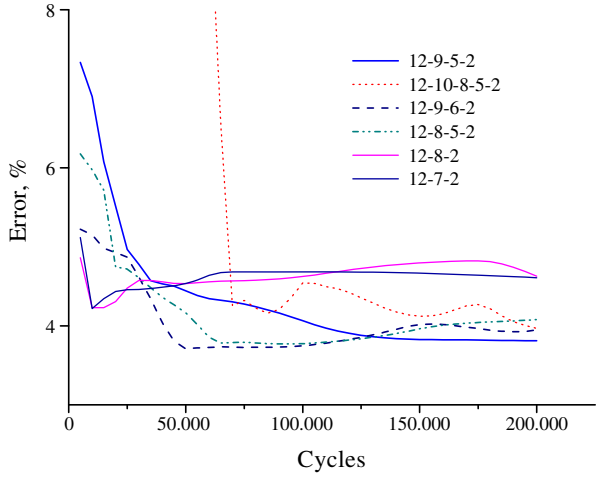

Fig. 7. Training histories of different ANN configurations.

The Nusselt number and friction factor trained by ANN 12-9-5-2 plotted against experimental data is shown in Fig. 8. The network is trained with 78% of experimental data as described earlier. It can be clearly seen that both predicted results trained by the 12-9-5-2 network are very close to the corresponding measured data. The maximum averaged relative error between the trained predictions and measured data is less than 5%, with an *rms* error of 1.44%. The prediction and the corresponding error of friction factor and Nusselt number of the heat exchangers by the ANN 12-9-5-2 is shown in Fig. 9. The straight line indicates perfect prediction. From the figure, it is found that the predictions of Nusselt number and friction factor close to the measured data well as the points approach the line closely. The maximum prediction error is also less than 5% with most of the errors being less than 2%. As listed in Table 2, $R = 1.000385$ and $\sigma = 0.004753$ suggest the good accuracy and scatter of the predictions. Accordingly, it should be noticed that the accuracy and the precision of predicted results are remarkable. The selection process of the network is similar to that in [33].

In Table 2, the errors by dimensionless power-law correlations from Tang et al. [34] are included. It is found from Table 2 that the errors of the correlations are much larger than those of the chosen ANN configuration. A comparison of prediction by ANN and power-law correlations is shown in Fig. 10. From the figure, it is observed that the predictions by correlations are not as good as those predictions by the 12-9-5-2 network. As examined in figure,

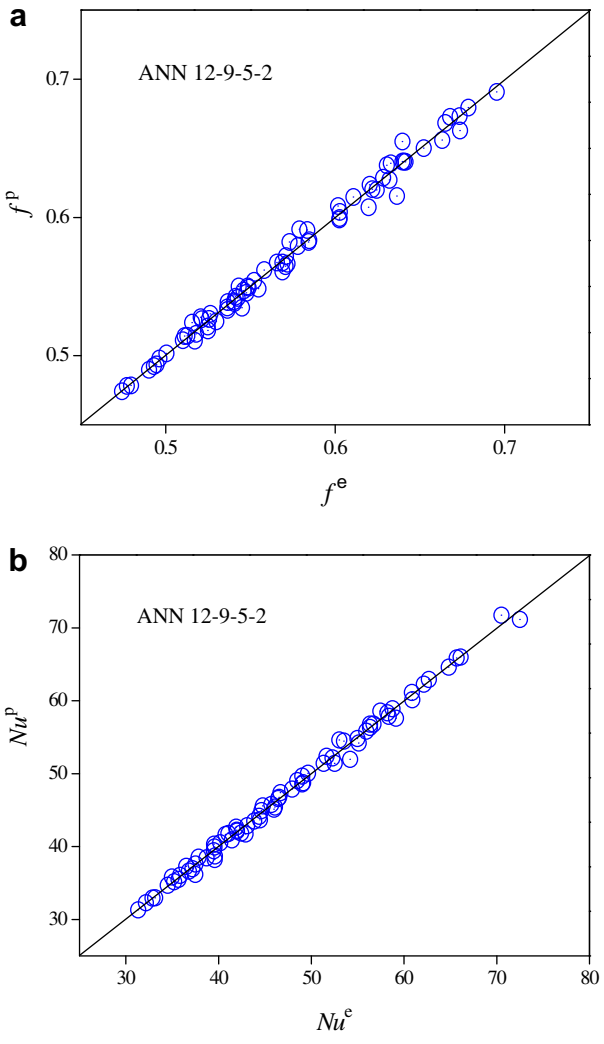

Fig. 8. Predictions of *Nu* and *f* by ANN with training data.

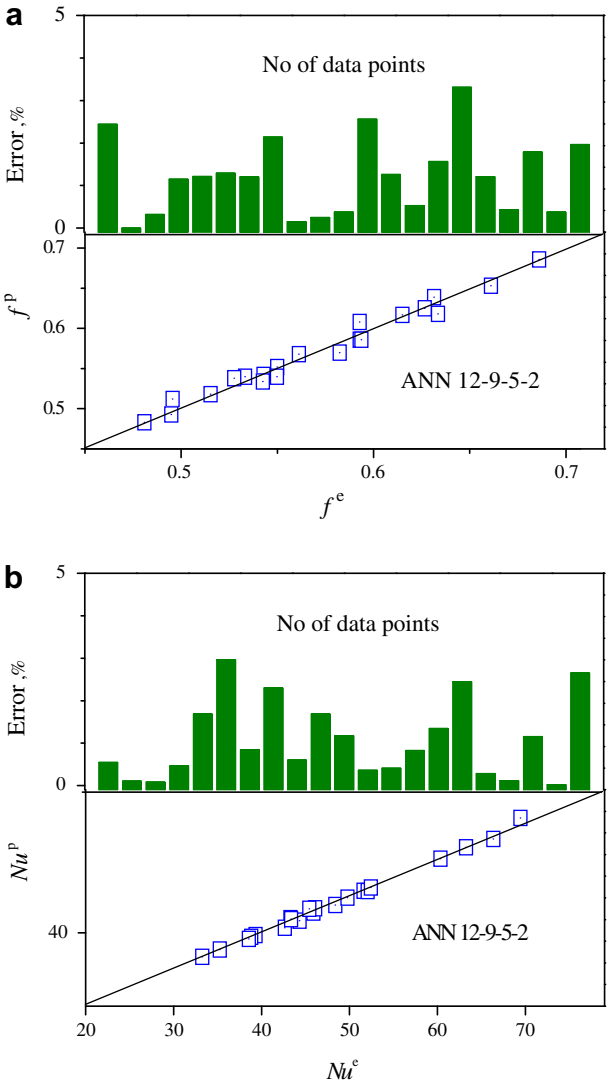

Fig. 9. Predictions of *Nu* and *f* by ANN with testing data.

most points of the prediction by ANN are close to the straight lines whereas most points of the prediction by correlations are slightly far from the lines. Therefore, for the presented heat exchangers at hand, ANN is superior to power-law correlations for prediction. Similar conclusions are also stated in [13,16,17,20–25].

5. Evaluation of ANN with CFD data

It is shown in the preceding section that the presented ANN configuration 12-9-5-2 can predict the heat exchanger performance well. Now independent data is used to evaluate this ANN, because the currently developed ANN is obviously satisfying the experimental data, of which most were used to train the ANN. In order to generalize the ANN 12-9-5-2 application, another database should be found for evaluation. Fortunately the data of heat exchangers with large number of tube rows and large tube-diameter has been provided through computational fluid dynamics (CFD) technique by Tang et al. [38]. Although the number of data sets is relatively small, the data can be used to test the ANN.

Tang et al. [38] used the commercial code FLUENT 6.1 for the numerical solution of the Navier–Stokes and energy equations using the standard two-equation $k - \varepsilon$ turbulence model. All variables, including velocity components, pressure and temperature

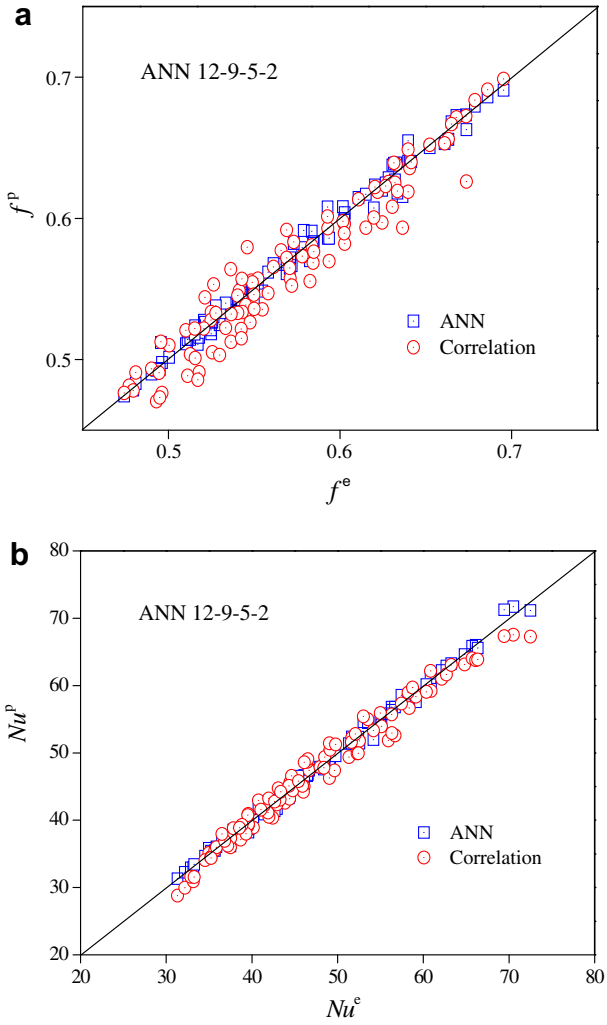

Fig. 10. Comparison of *Nu* and *f* predictions by ANN and power-law correlation.

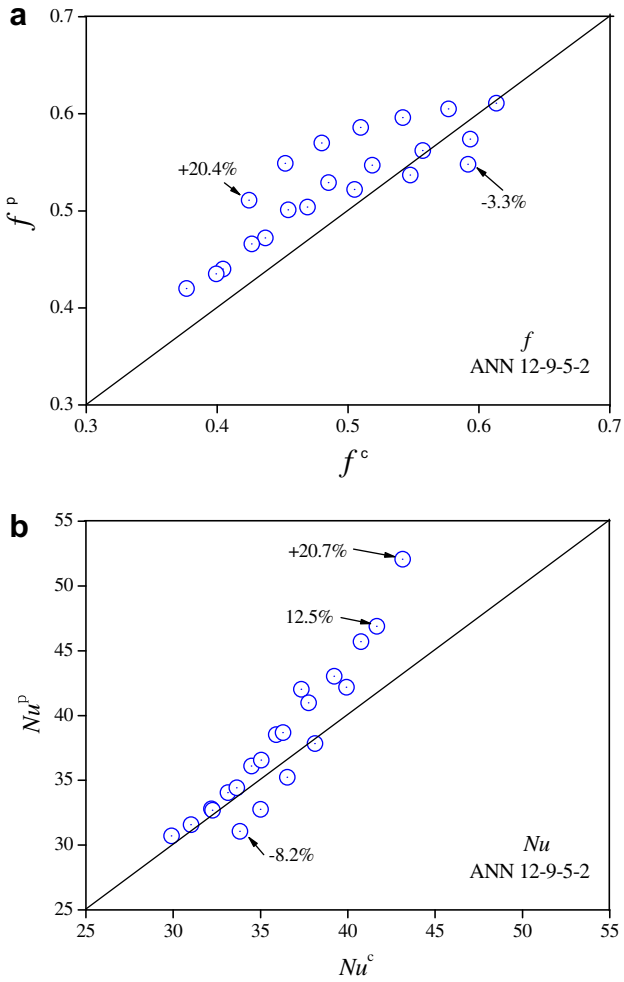

Fig. 11. Predictions of *Nu* and *f* by ANN trained with experimental data.

are averaged and applied to a control volume. The coupling between pressure and velocity is implemented by the SIMPLEC algorithm. It was shown that at moderate Reynolds number the mean deviation of *Nu* number is 6.0% with the maximum deviation being 15.8% and the mean deviation of *f* is 8.3% with the maximum deviation being 11.1% compared experimental data. It is worthwhile to note that for numerical simulation of heat transfer and friction factor characteristics, such an agreement between simulations and test results should be regarded satisfactory. Because in the simulations, the model is a perfect heat exchanger and many small details have been simplified. More details about the computations and results can be found in [38].

The evaluation of the ANN 12-9-5-2 configuration with the CFD data are shown in Fig. 11. From the observation of the two sub-figures it is shown that the neural network does not predict as well as experimental data. Much of the data is over-predicted by ANN with the maximum relative error being around 20%. However, most errors are below 10%. The results indicate differences between experimental data and computational data. This is supported by the fact that a small difference is presented in the geometries between experimental samples and geometrical size for computations. Without a clear advantage of the presented ANN with certain weights for predicting other models, suggests that it is necessary to combine experimental data and computational data to develop an integrated ANN with changing weights of the ANN internal connections. But for an engineering application, the currently trained ANN associated with its weights might be applied to predict the performance of heat exchangers, since the precision of the involved turbulence model with the CFD is also not guaranteed.

6. ANN trained with a combined database

6.1. Turbulent model of ANN

It is a very common way to get a "real" or "best" value by multiple measurements and computations. Thus if an ANN is trained with a database combining the experimental data and computational data, the network might provide a useful tool to predict the performance of such a kind of FTHEs with large number of tube rows and tube-diameter. To develop such a tool, the ANN 12-9-5-2 is now trained with the combined database including the previous experimental data used for selecting the ANN 12-9-5-2 and the numerical data by CFD. Here the numerical data is not only borrowed from the above database, as shown in Fig. 3, but also adopted from additional data through CFD computations [38,39], as used for validation of the network 12-9-5-2 in the preceding section. The prediction is shown in Fig. 12. From the figures, the predicted data is close to the experimental and numerical data. The R and σ of the ANN with the specific weights are 1.00322 and 0.00977. Also, the majority of predicted data points are less

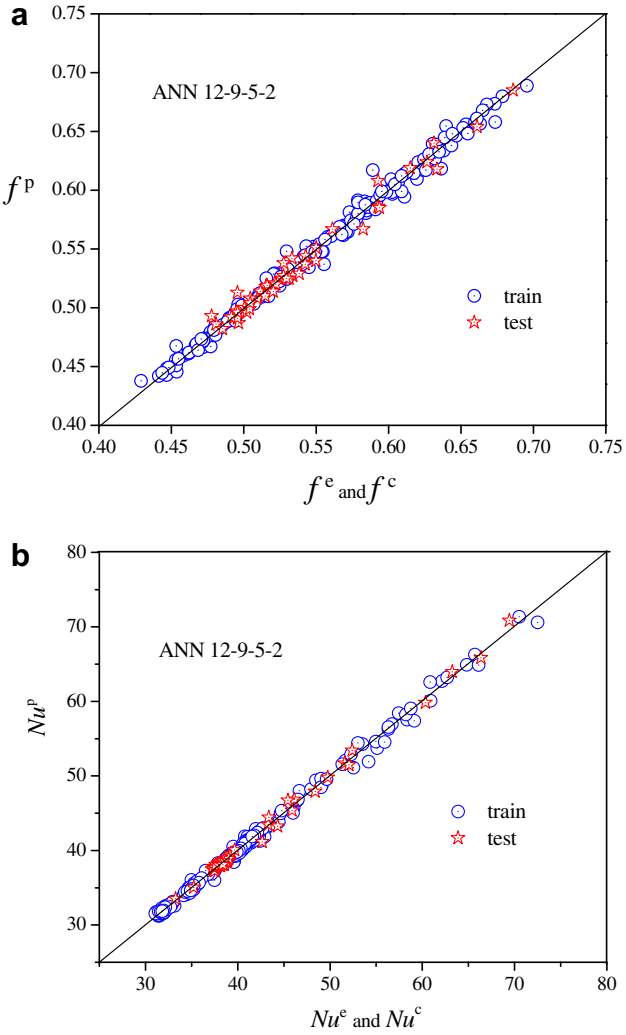

Fig. 12. Predictions of *Nu* and *f* by ANN with new weights and biases.

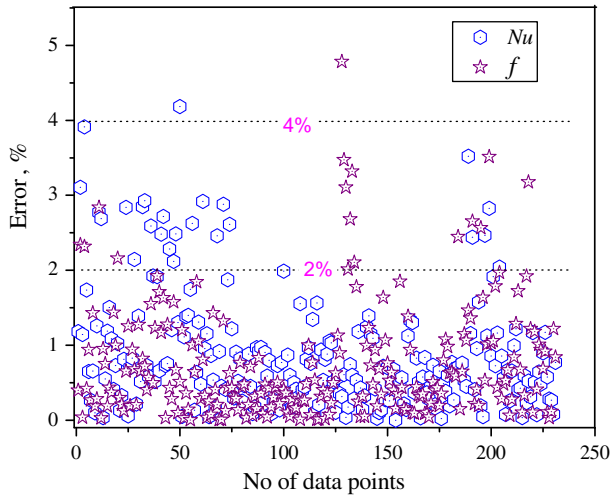

Fig. 13. Scatter distribution of relative errors from the predictions by the firstly-updated ANN.

than 5% from the combined data, as shown in Fig. 13. Therefore based on the presented prediction so far, the ANN 12-9-5-2 trained with the combined database of experimental and numerical data appears to be the "best" available prediction tool for obtaining turbulent flow and heat transfer for heat exchangers with large number of tube rows and large tube-diameter.

So for convenient use by engineers or researchers, the weights and biases under the ANN 12-9-5-2 are listed below. By inserting the sets of weights and biases, the turbulent flow and heat transfer of heat exchangers can be optimistically obtained. Thus at the present, the ANN is updated once with new weights and biases.

For the first layer, 108 weights and 9 biases are:

$$w_{12,9} = \begin{bmatrix} 9.70 & 3.18 & 4.34 & 6.55 & 0.75 & 2.82 & 7.72 & 7.18 & 4.58 \\ 6.94 & 0.43 & -6.61 & -0.93 & -6.80 & 5.93 & 2.74 & -1.31 & -7.61 \\ -1.35 & -0.57 & 0.98 & -1.53 & 1.16 & -4.04 & -1.96 & -1.04 & -2.21 \\ -1.32 & -0.54 & 1.01 & -1.50 & 1.19 & -4.01 & -1.93 & -1.01 & -2.19 \\ -1.35 & -0.57 & 0.98 & -1.53 & 1.16 & -4.04 & -1.96 & -1.04 & -2.21 \\ -1.32 & -0.54 & 1.01 & -1.50 & 1.19 & -4.01 & -1.93 & -1.01 & -2.19 \\ -2.55 & 0.52 & 0.15 & 0.34 & 0.01 & 0.00 & -0.49 & -0.10 & -1.08 \\ -2.52 & 0.55 & 0.19 & 0.37 & 0.04 & 0.03 & -0.46 & -0.07 & -1.04 \\ -2.55 & 0.52 & 0.15 & 0.34 & 0.01 & 0.00 & -0.50 & -0.10 & -1.08 \\ 1.62 & -1.70 & 2.63 & 1.39 & 13.24 & -6.96 & 1.49 & 1.99 & 8.90 \\ -3.71 & -3.67 & -3.61 & -1.67 & -5.38 & 7.47 & -2.77 & 0.13 & 1.70 \\ -1.73 & -2.94 & -7.10 & 2.14 & -18.18 & 12.88 & -2.26 & -0.48 & 2.66 \end{bmatrix},$$

$$b_9 = \begin{bmatrix} -2.67 \\ -1.12 \\ 1.99 \\ -3.03 \\ 2.36 \\ -8.05 \\ -3.90 \\ -2.05 \\ -4.40 \end{bmatrix}$$

For the second layer, 45 weights and 5 biases are:

$$w_{9,5} = \begin{bmatrix} 0.78 & -3.59 & -1.17 & 0.12 & 0.08 \\ -2.66 & -1.91 & -2.63 & 0.31 & -2.28 \\ 1.50 & -9.20 & 1.72 & 2.89 & -0.52 \\ -4.89 & 4.96 & -0.60 & -2.58 & -4.47 \\ -1.03 & 8.13 & -0.83 & -5.48 & 0.46 \\ -1.94 & -7.08 & 1.19 & -1.36 & -0.24 \\ -1.67 & -0.35 & 1.19 & -6.77 & -1.27 \\ 2.25 & 0.95 & -4.22 & 6.82 & -4.90 \\ 2.93 & 1.87 & 1.39 & -8.32 & -0.22 \end{bmatrix}, \quad b_5 = \begin{bmatrix} 1.84 \\ 1.71 \\ 2.22 \\ -0.84 \\ -0.84 \end{bmatrix},$$

For the third layer, 10 weights and 2 biases are:

$$w_{5,2} = \begin{bmatrix} -3.88 & -1.93 \\ -0.27 & 2.37 \\ -1.21 & 2.77 \\ -0.13 & 4.13 \\ -4.43 & 7.06 \end{bmatrix}, \quad b_2 = \begin{bmatrix} 4.08 \\ -3.17 \end{bmatrix}$$

6.2. Laminar and turbulent model for ANN

It must be recalled here that the so far firstly-updated ANN is suitable to predict the heat exchanger performance for turbulent heat transfer and fluid flow, and the experimental and

computational Reynolds number is in the range of 4000–10,000. However, as mentioned above, the generality is a very important feature of a well-established ANN. In the foregoing section, the turbulent model of the developed ANN is satisfactory for the conditions of turbulent flow and heat transfer. A heuristic question is raised: whether the above developed ANN 12-9-5-2 can be applied for laminar heat transfer and fluid flow at the low Reynolds numbers? In some particular situations the mass flow rate is low or the frontal area is so large that the entering velocity becomes small, and then the low Reynolds number appears and hence laminar flow and heat transfer is expected. On the other hand, turbulence with enhanced intensity of the heat transfer will generally lead to a dramatically increased pressure loss. The laminar condition for heat exchangers is sometimes designed in certain industrial application. Returning to the raised question and to answer it with explicitly, it is suggested that the testing work should be conducted. Fortunately, the authors [39,40] presented some numerical data for validation of the firstly-updated ANN.

In previous works of the authors, laminar flow and heat transfer of the presented heat exchangers were computed. The three-dimensional computations were carried out in Cartesian coordinates with the velocity–pressure coupling handled by the SIMPLE algorithm. The tube is assumed to be at constant temperature because the large heat transfer coefficient inside the tube and that the thermal conductivity of the tube wall is high while a low heat transfer coefficient prevails at the fins outside the tubes. But the temperatures in fin and solid are computed simultaneously under a conjugated manner. The effects of Reynolds number, the number of tube rows, tube-diameter, tube pitches are observed so that the corresponding data is picked up from these effects. Now these data is first for testing the ANN 12-9-5-2. The computational Reynolds number is ranged from 1000 to 6000 with frontal velocity being 0.47 to 4 m/s. More details of the computations can be found in Xie et al. [39,40]. Also, in those works the multiple correlations of the Nusselt number and friction factor are provided with the averaged deviations being 3.7% and 6.5%, respectively. These correlations are listed follows for later comparisons.

$$Nu = 1.565Re^{0.3414}\left(N_t \cdot \frac{F_p}{D_o}\right)^{-0.165}\left(\frac{P_t}{P_l}\right)^{0.0058} \tag{10a}$$

$$f = 20.713Re^{-0.3489}\left(N_t \cdot \frac{F_p}{D_o}\right)^{-0.168}\left(\frac{P_t}{P_l}\right)^{0.6562} \tag{10b}$$

Having picked up the database, the test work is now carried out. Since predictions can be directly obtained by feeding the inputs, the corresponding parameters of the numerical computations are input into the firstly-updated 12-9-5-2 network. The prediction is plotted in Fig. 14. It is apparently concluded that the predictions of the Nusselt number and hence the heat transfer, as well as the friction factor and hence the flow resistance are far from the computational database. Most over-predictions for the friction factor and most under-predictions for the Nusselt number are resulted. The outcome suggests a substantial difference between the turbulent and laminar convective heat transfer. The conclusion of the predictions is supported by the fact that the so far developed ANN is only trained and tested with databases of experimental and computational turbulent flow and heat transfer, and thereby no information of laminar flow and heat transfer is learned and stored in the neural network. This is to show the operation principle of the artificial neural network. No related database for learning the mechanism will lead to ANN's inability of outputting the needed message. Therefore, the answer is that the currently developed ANN can not predict laminar flow heat transfer in heat exchangers well.

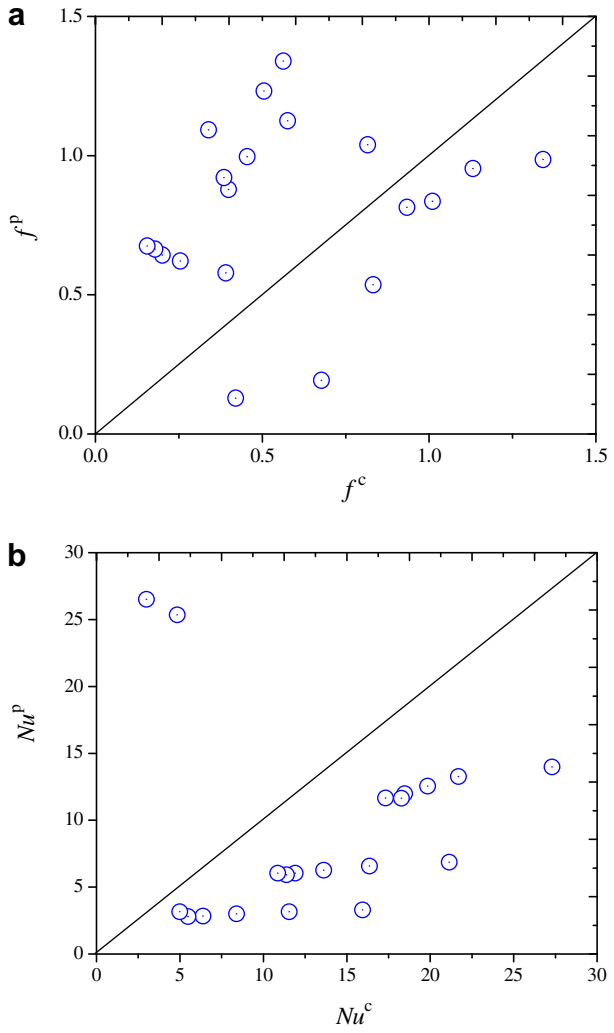

Fig. 14. Predictions of *Nu* and *f* by ANN with turbulent database.

The desire to predict laminar convective heat transfer implies the need updating the ANN a second time. In a similar way as above using, a new database for training and testing the neural network 12-9-5-2 is created by all the databases for turbulent and laminar flow and heat transfer. Totally, two hundreds and seventy-seven sets of data points are obtained. Among these, 190 sets of data points are for training the 12-9-5-2 secondly while the remaining ones are for testing the generality. The trained Nusselt number and friction factor by the ANN 12-9-5-2 are plotted against the combined database in Fig. 15. It is seen that both the trained results by the 12-9-5-2 network are close to corresponding data. The prediction of the friction factor and Nusselt number for the heat exchangers by the secondly-updated ANN 12-9-5-2 is shown in Fig. 16. The straight line means that the prediction is perfect and the dotted lines mean a deviation of 10%. From the figure, it is found that all the predictions of the Nusselt number is within a deviation of 10% and the majority (92%) of the predictions of the friction factor is also within a deviation of 10%. By careful examination, it is found that most of the predictions are within 4% deviation from the database, as shown in Fig. 17. The scatter distribution of the deviations shows good agreement with an accepted error less than 5%. It must be pointed out that in some situations the measurements and hence the uncertainties or computations have certain errors, sometimes up to 10%, or 20%

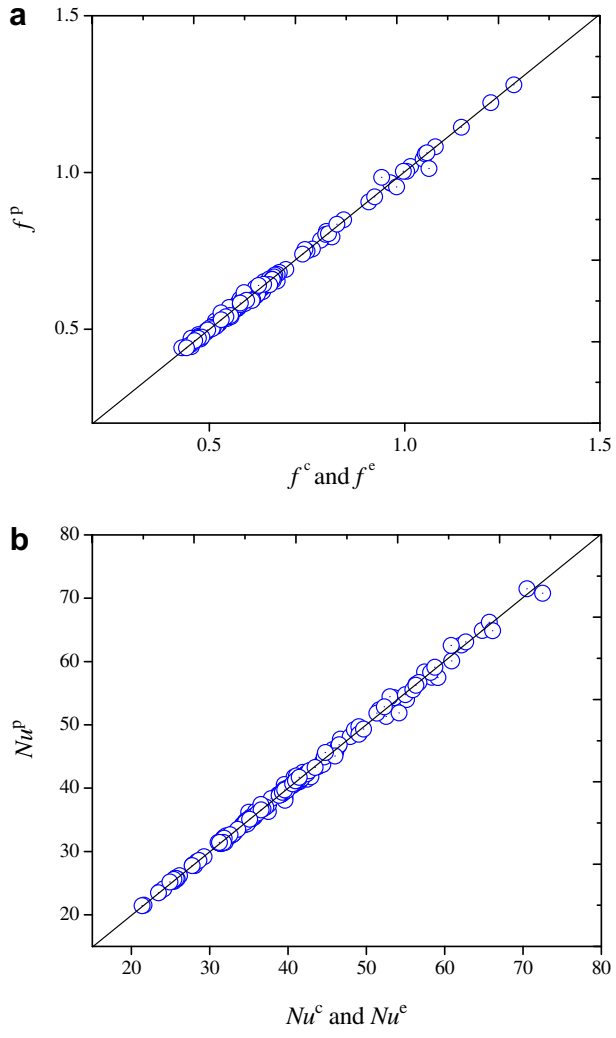

Fig. 15. Trained *Nu* and *f* by secondly-updated ANN.

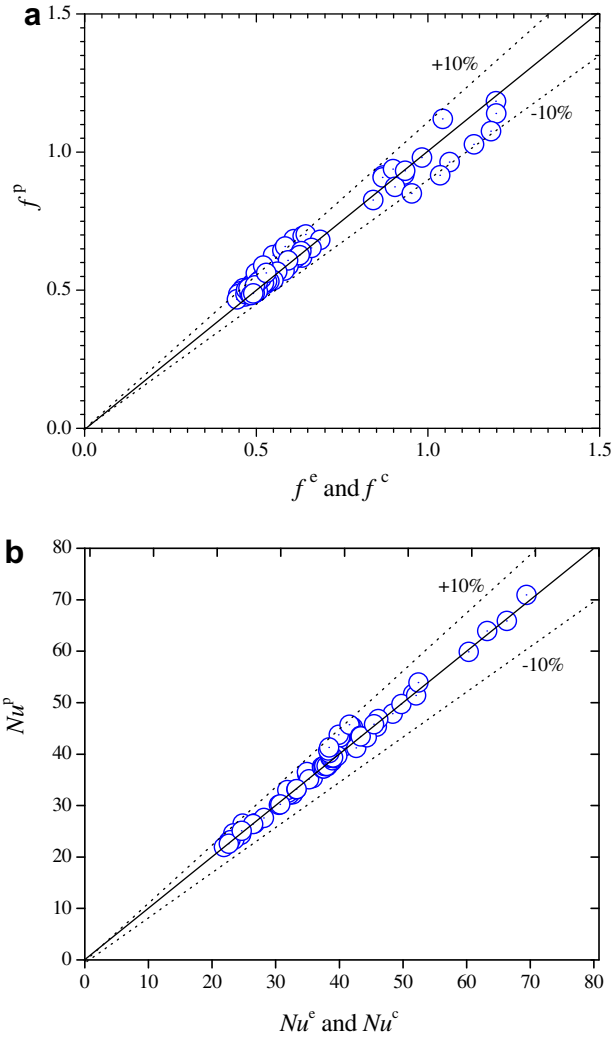

Fig. 16. Predictions of *Nu* and *f* by ANN with combined data from laminar and turbulent heat transfer and fluid flow data. The dotted lines mean a deviation of 10%.

for turbulent computations. The predictions here reflect this inaccuracy in the database because the predictions are of course not better than the perfect measurements or computations. Consequently, the secondly-updated 12-9-5-2 is now used for prediction of laminar and turbulent flow and heat transfer performance of the presented heat exchangers having large number of tube rows and tube-diameter.

In order to again show the confidence that the artificial neural network approach is superior to correlations for predictions, the comparison is plotted in Fig. 18. Since the comparison based on the database for turbulent flow and heat transfer was shown in previous section, only the database from laminar flow and heat transfer is used here for this comparison. It can be seen that the predictions by ANN are better than those by multiple correlations, Eq. (8). The average errors of *f* and *Nu* are 3.84% and 1.85%, respectively. So, the conclusion that the ANN is superior compared to correlations for prediction of the presented heat exchanger is now supported again.

Also, for convenient use by engineers or researchers, the weights and biases for secondly-updated ANN 12-9-5-2 are listed below. The sets of weights and biases can be directly read into the network by an encoded program so that the turbulent and laminar convective heat transfer of the heat exchangers can be obtained. Thus two sets of weights and biases are provided here for future research works.

For the first layer, 108 weights and 9 biases are:

$$w_{12,9} = \begin{bmatrix} 0.40 & 1.47 & 4.43 & 5.70 & 12.00 & -5.74 & 8.12 & 5.26 & 4.20 \\ -0.85 & 1.78 & 0.67 & -3.96 & 0.39 & -3.72 & 16.75 & -6.66 & 9.40 \\ -5.52 & 0.37 & -2.59 & 0.72 & -2.33 & 0.69 & 0.04 & 0.24 & -3.01 \\ 13.38 & -0.75 & 7.85 & -0.77 & -0.81 & 5.51 & 2.11 & -3.72 & -2.16 \\ -1.96 & -0.91 & -0.20 & 0.96 & -2.64 & -0.62 & 0.56 & -1.64 & -3.21 \\ 4.75 & -1.24 & -1.27 & -0.95 & -0.55 & 0.79 & -0.19 & -1.69 & -3.12 \\ 0.82 & 0.88 & -0.53 & 0.98 & -1.51 & 0.68 & -0.18 & 2.63 & -0.48 \\ 0.85 & 0.92 & -0.50 & 1.01 & -1.48 & 0.71 & -0.14 & 2.66 & -0.45 \\ 0.82 & 0.88 & -0.53 & 0.98 & -1.51 & 0.68 & -0.18 & 2.63 & -0.48 \\ -2.43 & -1.49 & 2.06 & -2.05 & -0.91 & 0.37 & -0.46 & -1.91 & 0.82 \\ 1.38 & 1.72 & -1.12 & -2.58 & -3.61 & 1.55 & -2.13 & -1.66 & 3.02 \\ 1.35 & 0.14 & -1.08 & 3.70 & -3.31 & -0.51 & -1.28 & 0.33 & -0.87 \end{bmatrix},$$

$$b_9 = \begin{bmatrix} -3.15 \\ -0.74 \\ -4.66 \\ 2.69 \\ -0.65 \\ 4.19 \\ -3.57 \\ 1.16 \\ 0.45 \end{bmatrix}$$

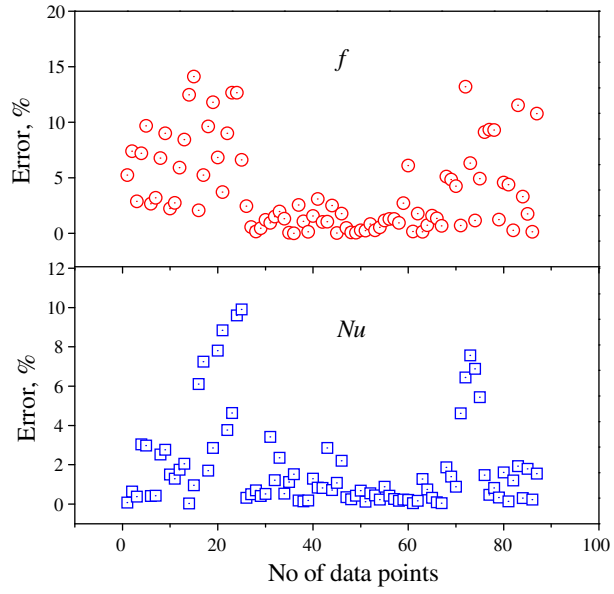

Fig. 17. Scatter distribution of relative errors from the predictions by the secondly-updated ANN.

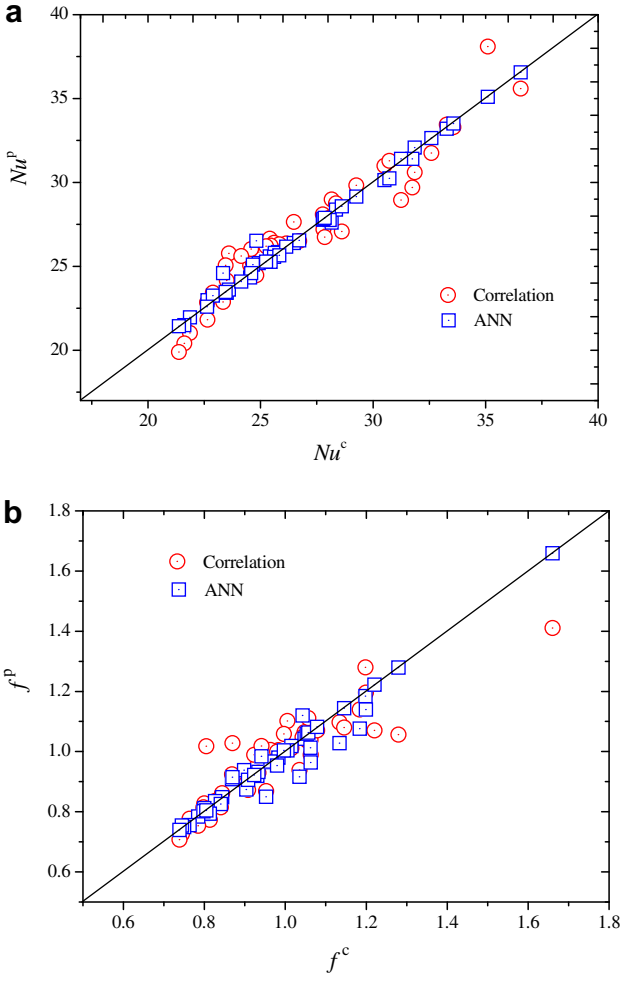

Fig. 18. Comparison of *Nu* and *f* predictions by ANN and multiple correlations [40].

For the second layer, 45 weights and 5 biases are:

$$w_{9,5}=\begin{bmatrix} 1.22 & -7.12 & -1.74 & -6.05 & -2.06 \\ -2.14 & 0.76 & -0.79 & 0.17 & -4.71 \\ 2.95 & -2.35 & 0.81 & 2.55 & -2.21 \\ -2.71 & -0.88 & -0.88 & -2.75 & -3.29 \\ -2.14 & 0.37 & -6.07 & -3.08 & 2.55 \\ -0.88 & 1.62 & -1.39 & 0.30 & 2.70 \\ 4.32 & 6.67 & -3.03 & 2.01 & 0.00 \\ -4.50 & 3.06 & -0.83 & 0.05 & 2.21 \\ -6.27 & -1.76 & -3.93 & -0.06 & -1.44 \end{bmatrix}, \quad b_5=\begin{bmatrix} 1.70 \\ -3.85 \\ -2.75 \\ -5.44 \\ -1.11 \end{bmatrix}$$

For the third layer, 10 weights and 2 biases are:

$$w_{5,2}=\begin{bmatrix} -3.99 & 4.09 \\ -2.92 & -1.04 \\ -6.22 & -0.57 \\ -2.84 & 3.47 \\ -8.19 & 1.19 \end{bmatrix}, \quad b_2=\begin{bmatrix} 4.97 \\ -1.78 \end{bmatrix}$$

Here we again present the application geometrical ranges for heat exchanger having large tube-diameter and large number of tube rows:

$Re_{D_c} = 1000$–$10,000$, D_o = 16–20 mm, N_t = 2–12,
F_p = 2–4 mm, P_t = 38–46 mm, P_l = 32–36 mm.

7. Discussion

The users can input the above listed weights and biases into the specific artificial neural network configuration, in turn to predict the corresponding performance of heat exchangers when the geometrical parameters are input to the network. The currently predicted results indicate that the developed ANN might be extended to predict heat exchanger performance well for different sets of input data of specific heat exchangers.

The reason for selection of a single ANN to prediction turbulent and laminar flow and heat transfer is now discussed. The authors have separated laminar data to train ANN, and the result of the predicted error is shown in Fig. 19. Compared to Fig. 17, it is recognized that by only using laminar data for training ANN results in maximum errors of the same level as by using combined laminar and turbulent data. Although the mixed data slightly reduce the

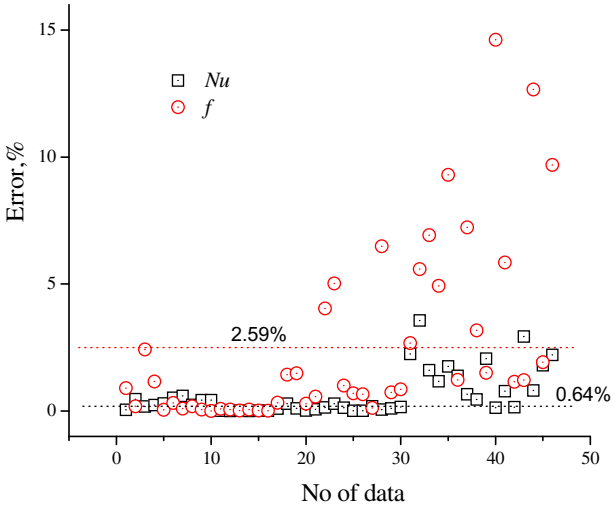

Fig. 19. Prediction errors from ANN with laminar data (only laminar data is used for training the ANN).

Table 3
Prediction errors from ANN and correlations, %.

	ANN with turbulent data	ANN with laminar data	ANN with combined database	Power-law correlations Eqs. (1–3), Tang et al. [34]	Multiple correlations Eq. (10), Xie et al. [40]
Nu	0.88	0.64	1.85	6.5	3.7
f	0.73	2.59	3.84	8.7	6.5

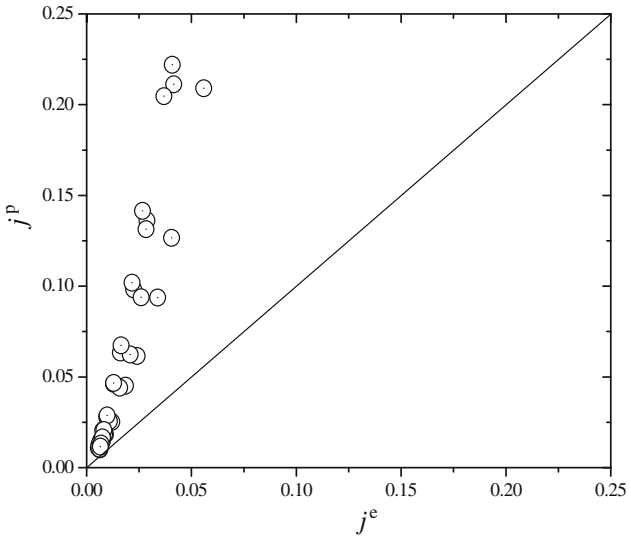

Fig. 20. Prediction from the present ANN against experimental data of Wang et al. [5].

accuracy of the secondly-updated ANN, superiority compared to correlations is achieved, as supported by Fig. 18. For multiple correlations, the average errors of *f* and *Nu* are 6.5% and 3.7%, respectively. The prediction errors from ANN and correlations are listed in Table 3. The reasons of combining laminar and turbulent data for training the ANN are that the flow inside the heat exchanger passages is complex and no sufficient experimental data exist to judge whether the flow is laminar or turbulent, and the number of laminar data is evidently small compared to the number of turbulent data (46 and 231, respectively). In most conditions turbulent flow and heat transfer occur in heat exchanger applications, hence one may apply the single ANN for prediction or heat exchanger design.

Another issue is the possibility of extending the present ANN to predict performance of heat exchangers with small tube-diameter and tube-row. This is addressed here. A typical prediction is plotted in Fig. 20. The experimental data is picked up from Fig. 3 of Wang et al. [5]. It is clearly seen that severe over-prediction occurs, indicating that a non-satisfactory result is obtained. This result is supported by the fact that the developed ANN did not learn anything about the heat exchangers with small values of tube-diameter and tube-row. In Wang et al. [5], the outside diameter of tube and the number of tube rows are 10 mm and 1 or 2, respectively. Since fin-and-tube heat exchangers studies are numerous with different geometries, the authors do not and can not collect all information about fin-and-tube heat exchangers for ANN prediction. Therefore, the present work is limited to application of ANN for such kind of heat exchangers having large tube-diameter and large number of tube rows, and contributes to successful application of ANN in thermal sciences.

Improving heat exchanger design is an active research field for thermal designers. There are many experimental and numerical studies on design of heat exchangers. However, it is generally difficult to collect all the data for design, because the extensive costs of experiments (including costs for setups and manufacturing samples) and the computer resources for computations. Therefore, the use of different methods can be considered as alternative techniques for design. The ANN approach is useful and convenient for engineers or researchers to predict the performance of a given heat exchanger with limited experimental data. It does not need to provide an accurate and detailed mathematical formulation. Once the ANN was trained, the weights and biases from the network, which correspond to a practical heat exchanger, can be transferred to engineers or researchers who are going to use the tested data for prediction. Then engineers may simply feed these data into the trained network and therefore quickly make accurate predictions of the thermal performance for the practical heat exchanger. However, some limitation should be considered from ANNs, since they do not provide any knowledge about the physical phenomena and do not correlate the information. That is, ANN does not know the inherent physical principle, and how and why the phenomena occur, or change, or disappear.

8. Conclusions

In the present work various neural network configurations have been tested based on experimentally measured databases of Nusselt number and friction factor of three kinds of heat exchangers. It is concluded that the 12-9-5-2 feed-forward neural network is the most accurate architecture for prediction of turbulent heat transfer and flow resistance for the fin-and-tube heat exchangers having plain fins, slit fins and fins with longitudinal vortex generators with large tube-diameter and large number of tube rows. Also the presented ANN yields the superior prediction of heat transfer and flow friction compared to power-law or multiple correlations.

By extension to train the ANN for the combined database from experimental data and numerical data by computational fluid dynamics (CFD) technique, the developed ANN architecture is more exactly generalized and universal. Therefore the ANN 12-9-5-2 architecture behaves strong ability to predict of heat exchanger performance of turbulent and laminar heat transfer and fluid flow with an accepted deviation close to the measurement uncertainty/error.

The weights and biases of ANN 12-9-5-2 corresponding to turbulent or laminar model are also provided in this paper so that the engineering applications or further researches can be carried out. The ultimate ANN will be trained with more and more accurately measured or computed data from more heat exchangers and then will be able to predict heat transfer and flow resistance much better. Consequently, the presented ANN in this study is well suitable for prediction laminar or/and turbulent heat transfer and fluid flow of such kinds of heat exchangers and for heat transfer analysis. But it must be remembered that the limitation of ANN is that it can not describe the unknown physical phenomena directly.

Acknowledgments

This work is supported by National Nature Science Foundation of China (No. 50521604) and Program for New Century Excellent Talents in University (NCET-04-0938).

References

[1] R.K. Shah, D.P. Sekulic, Fundamentals of Heat Exchanger Design, John Wiley, London, UK, 2003.
[2] R.L. Webb, N.-H. Kim, Principles of Enhanced Heat Transfer, second ed., Taylor & Francis Group, New York, 2005.
[3] B. Sundén, Computational fluid dynamics in research and design of heat exchangers, Heat Transfer Eng. 28 (2007) 898–910.
[4] C.C. Wang, Recent progress on the air-side performance of fin-and-tube heat exchangers, Int. J. Heat Exchangers 2 (2000) 57–84.
[5] C.C. Wang, K.Y. Chi, Heat transfer and friction characteristics of plate fin-and-tube heat exchangers. Part I: new experimental data, Int. J. Heat Mass Transfer 43 (2000) 2681–2691.
[6] C.C. Wang, K.Y. Chi, C.J. Chang, Heat transfer and friction characteristics of plate fin-and-tube heat exchangers. Part II: correlation, Int. J. Heat Mass Transfer 43 (2000) 2693–2700.
[7] C.C. Wang, W.S. Lee, W.J. Sheu, A comparative study of compact enhanced fin-and-tube heat exchangers, Int. J. Heat Mass Transfer 44 (2001) 3565–3573.
[8] J.S. Leu, Y.H. Wu, J.Y. Jang, Heat transfer and fluid flow analysis in plate-fin and tube heat exchangers with a pair of block shape vortex generators, Int. J. Heat Mass Transfer 47 (2004) 4327–4338.
[9] B. Sundén, M. Faghri, Computer Simulations in Compact Heat Exchangers, Computational Mechanics, Inc., UK, 1998.
[10] M. Sen, K.T. Yang, Applications of artificial neural networks and genetic algorithms in thermal engineering, in: F. Kreith (Ed.), The CRC Handbook of Thermal Engineering, CRC Press, Boca Raton, FL, 2000.
[11] K.T. Yang, M. Sen, Artificial neural network-based dynamic modeling thermal systems and their control, in: B.X. Wang (Ed.), Heat Transfer Science and Technology, Higher Education Press, Beijing, 2000.
[12] G. Diaz, M. Sen, K.T. Yang, R.T. McClain, Simulation of heat exchanger performance by artificial neural networks, Int. J. HVAC&R Res. 5 (1999) 195–208.
[13] G. Diaz, M. Sen, K.T. Yang, R.T. McClain, Dynamic prediction and control of heat exchangers using artificial neural networks, Int. J. Heat Mass Transfer 45 (2001) 1671–1679.
[14] G. Diaz, M. Sen, K.T. Yang, R.T. McClain, Adaptive neuro-control of heat exchangers, ASME J. Heat Transfer 123 (2001) 417–612.
[15] G. Diaz, M. Sen, K.T. Yang, R.T. McClain, Stabilization of thermal neuro-controllers, Appl. Artif. Intell. 18 (2004) 447–466.
[16] A. Pacheco-Vega, G. Diaz, M. Sen, K.T. Yang, R.T. McClain, Neural network analysis of fin-tube refrigerating heat exchanger with limited experimental data, Int. J. Heat Mass Transfer 44 (2000) 763–770.
[17] A. Pacheco-Vega, G. Diaz, M. Sen, K.T. Yang, R.T. McClain, Heat rate predictions in humid air–water heat exchangers using correlations and neural networks, ASME J. Heat Transfer 123 (2001) 348–354.
[18] Y. Islamoglu, A new approach for the prediction of the heat transfer rate of the wire-on-tube type heat exchanger-use of an artificial neural network model, Appl. Thermal Eng. 23 (2003) 243–249.
[19] Y. Islamoglu, A. Kurt, C. Parmaksizoglu, Performance prediction for non-adiabatic capillary tube suction line heat exchanger: an artificial neural network approach, Energy Conversion Manag. 46 (2005) 223–232.
[20] G.N. Xie, Q.W. Wang, M. Zeng, L.Q. Luo, Heat transfer analysis for shell-and-tube heat exchangers with experimental data by artificial neural networks approach, Appl. Thermal Eng. 27 (2007) 1096–1104.
[21] Q.W. Wang, G.N. Xie, M. Zeng, L.Q. Luo, Prediction of heat transfer rates for shell-and-tube heat exchangers by artificial neural network approach, J. Thermal Sci. 15 (2006) 257–262.
[22] H.M. Ertunc, M. Hosoz, Artificial neural network analysis of a refrigeration system with an evaporative condenser, Appl. Thermal Eng. 26 (2006) 627–635.
[23] M. Hosoz, H.M. Ertunc, H. Bulgurcu, Performance prediction of a cooling tower using artificial neural network, Energy Conversion Manag. 48 (2007) 1349–1359.
[24] K.S. Yigit, H.M. Ertunc, Prediction of the air temperature and humidity at the outlet of a cooling coil using neural networks, Int. Commun. Heat Mass Transfer 33 (2006) 898–907.
[25] G.J. Zdaniuk, L.M. Chamra, D.K. Walters, Correlating heat transfer and friction in helically-finned tubes using artificial neural networks, Int. J. Heat Mass Transfer 50 (2007) 4713–4723.
[26] Y. Islamoglu, A. Kurt, Heat transfer analysis using ANNs with experimental data with air flow in corrugated channels, Int. J. Heat Mass Transfer 47 (2004) 1361–1365.
[27] A.J. Ghajar, L.M. Tam, S.C. Tam, Improved heat transfer correlation in transition region for a circular tube with three inlet configurations using artificial neural networks, Heat Transfer Eng. 25 (2) (2004) 30–40.
[28] S.S. Sablani, A. Kacimov, J. Perret, A.S. Mujumdar, A. Campo, Non-iterative estimation of heat transfer coefficients using artificial neural network models, Int. J. Heat Mass Transfer 48 (2005) 665–679.
[29] S. Deng, Y. Hwang, Applying neural networks to the solution of forward and inverse heat conduction problems, Int. J. Heat Mass Transfer 49 (2006) 4732–4750.
[30] S. Deng, Y. Hwang, Solution of inverse heat conduction problems using Kalman filter-enhanced Bayesian back propagation neural network data fusion, Int. J. Heat Mass Transfer 50 (2007) 2089–2100.
[31] K. Ermis, A. Erek, I. Dincer, Heat transfer analysis of phase change process in a finned-tube thermal energy storage system using artificial neural network, Int. J. Heat Mass Transfer 50 (2007) 3163–3175.
[32] B. Ayhan-Sarac, B. Karlık, T. Bali, T. Ayhan, Neural network methodology for heat transfer enhancement data, Int. J. Numer. Methods Heat Fluid Flow 17 (2007) 788–798.
[33] G.N. Xie, L.H. Tang, B. Sunden, Q.W. Wang, Artificial neural network based correlating heat transfer and friction factor of fin-and-tube heat exchanger with large number of large-diameter tube rows, in: Proceedings of 2008 ASME Heat Transfer Conference, August 10–14, 2008, Jacksonville, Florida, USA, ASME HT2008-56241.
[34] L.H. Tang, M. Zeng, G.N. Xie, Q.W. Wang, Fin pattern effects on air-side heat transfer and friction characteristics of fin-and-tube heat exchangers with large number of large-diameter tube rows, Heat Transfer Eng. 30 (2009) 171–180.
[35] L.H. Tang, G.N. Xie, M. Zeng, Q.W. Wang, A comparative study of fin-and-tube heat exchangers with various fin patterns, in: Proceedings of GT2008, ASME Turbo Expo 2008, May 8–11, 2008, Berlin, Germany, GT2008-51504.
[36] L.H. Tang, G.N. Xie, M. Zeng, X.H. Yan, H.G. Wang, Q.W. Wang, Experimental investigation on heat transfer and flow friction characteristics in three types of plate fin-and-tube heat exchangers, J. Xi'an Jiaotong Univ. 41 (2007) 521–525 (in Chinese).
[37] S. Haykin, Neural Networks: A Comprehensive Foundation, Prentice Hall, NJ, Upper Saddle River, 1999.
[38] L.H. Tang, G.N. Xie, M. Zeng, M. Lin, Q.W. Wang, Numerical simulation of fin patterns on air-side heat transfer and flow friction characteristics of fin-and-tube heat exchangers, in: Proceedings of ASCHT07, 1st Asian Symposium on Computational Heat Transfer and Fluid Flow, October 18–21, Xi'an, China, 2007, Paper No. 2007-109.
[39] G.N. Xie, Improvements of fin-and-tube heat exchangers and their design optimizations, Ph.D. thesis, School of Energy and Power Engineering, Xi'an Jiaotong University, 2007/09 (in Chinese).
[40] G.N. Xie, Q.W. Wang, B. Sundén, Parametric study and multiple correlations of heat transfer and fluid flow characteristics of fin-and-tube heat exchanger with large number of large-diameter tube rows, Appl. Thermal Eng. 29 (2009) 1–16.